Predefinable colorimetric quantum-dot barcodes with simple and express identification algorithm

Bo Wu and Hai-Qing Gong*

School of Mechanical & Aerospace Engineering, Nanyang Technological University, 50 Nanyang Avenue, Singapore 639798, Singapore

*Corresponding author: MHQGONG@ntu.edu.sg

Received 11 September 2012; revised 26 November 2012; accepted 22 December 2012; posted 4 January 2013 (Doc. ID 175703); published 1 February 2013

Specific fluorescent profiles were created by loading quantum-dot (Qdot) mixtures in liquid cores of monodispersed polymer microcapsules, which were used as colorimetric barcodes for small object identification. Since the emission intensities of Qdot-loaded liquid cores maintain a linear relation to the Qdot concentrations and the Qdots in the liquid cores with different emission peaks have no obvious interference, the colorimetric barcodes can be predefined by the compositions of Qdot mixtures. The colorimetric barcodes can be identified easily by recording the emission intensities of the encoded microcapsules at respective Qdot emission peaks with a simple and express algorithm, which are suitable to conduct high-throughput multiplexed assays by flow cytometer for biological screening applications. © 2013 Optical Society of America

OCIS codes: 160.2540, 070.4790, 230.0040.

1. Introduction

Quantum-dots (Qdots) are semiconductor nanocrystals with high photostability, narrow emission bands, and high quantum efficiencies, which are used as alternates to conventional organic fluorescent dyes for imaging, labeling, and sensing applications [1,2]. The Qdot emission peaks can be controlled by their sizes during synthesis. The Qdots with different emission peaks can be excited simultaneously by UV light. Taking these advantages of Qdots, Han *et al.* proposed a concept of using the Qdots to create colorimetric barcodes to conduct multiplexed bioassays [3]. The barcodes are formed by embedding the Qdots with different emission peaks over the outer surfaces of polymer microparticles in controlled ratios, which can emit specific fluorescent profiles for identifying the biomolecules immobilized on the encoded microparticles. Plenty of bioassays can be conducted simultaneously by tracking the barcodes for drug discovery, gene profiling, and clinic diagnostics. The barcodes can also be formed by coating the Qdots over the outer surfaces of microparticles by layer-by-layer self-assembly [4]. The above two methods to fix the Qdots at the outer surfaces of microparticles have drawbacks including the leakage of Qdots to ambient fluids and unstable fluorescent profiles in different bioassay buffers [5]. To circumvent these problems, the microparticles doped with the Qdots internally are made by solidifying the polymer precursor droplets mixed with the Qdots [6]. However, the fluorescence resonance energy transfer (FRET) due to the aggregation of the Qdots in the polymer matrix and the shrinkage of microparticles upon the polymerization cause the fluorescent profiles of the Qdot-doped microparticles to be unpredictable, which requires further interrogation to check their specificities as unique barcodes.

We developed colorimetric barcodes formed in monodispersed microcapsules in size of 30 μm [7]. The microcapsules with liquid cores and transparent polymer shells are templated from microfluidic double emulsion droplets [8–10]. By loading the Qdots in the liquid cores, stable and repeatable colorimetric barcodes are formed with predefined fluorescent profiles. The barcode formation process is highly

1559-128X/13/040866-05$15.00/0

simplified by multiplexing the Qdot emission peaks and concentrations in the liquid cores. Each specific Qdot mixture can create a specific fluorescent profiles as a barcode. Here we demonstrate the identification of the colorimetric barcodes by recording the emission intensities of encoded microcapsules at the Qdot emission peaks by a CCD camera and narrow bandpass optical filters under a microscope. A simple and express algorithm is used to calculate the relative compositions of Qdot mixtures, which are used as barcodes. Because of the simplicity of the identification algorithm used, the predefinable colorimetric barcodes are suitable to conduct high-throughput multiplexed assays by flow cytometer for biological screening applications [11,12].

2. Preparation of Microcapsules

A microfluidic device was made by soft lithograph of polydimethylsiloxane [13] to fabricate the Qdot-encoded microcapsules. As illustrated in Fig. 1(a), the microfluidic device consists of a T-junction, a Y-junction, and a serpentine section. The microcapsules are fabricated in three steps. First, Qdot-solution droplets are generated at the T-junction and suspended in a flow of ethoxylated trimethylolpropane triacrylate (ETPTA) polymer precursor [Fig. 1(b)]. Second, the Qdot-solution droplets are engulfed inside larger droplets of the ETPTA polymer precursor at the Y-junction to form the double emulsion droplets in a flow of 2% sodium dodecyl sulfate (SDS) solution [Fig. 1(c)]. Finally, the ETPTA droplets are solidified by UV light to form the microcapsules in the serpentine section [Fig. 1(d)]. The Qdot solutions to form the Qdot-loaded liquid cores were prepared by dispersing water-dispersible CdTe Qdots in deionized water. The Qdot emission peaks are at 550 nm (Qdot550), 600 nm (Qdot600), and 650 nm (Qdot650). The molar concentrations of the Qdots were measured and calibrated based on Lambert–Beer's law with the Qdots' absorbances and extinction coefficients at their first excitons [14], which were measured by a UV–vis spectrophotometer (UV-2450, Shimadzu, Japan). The ETPTA polymer precursor was prepared by dissolving 2% surfactant of sorbitan monooleate (Span80) and 4% photoinitiator of Daracure 1173 in ETPTA monomer. The Qdot solution, the ETPTA polymer precursor, and the SDS solution were injected into the microfluidic device by three syringe pumps individually.

The sizes of the Qdot-solution droplet and the ETPTA droplet were controlled precisely by the flow rates of above three fluids independently. Generally speaking, the higher flow rate of ETPTA polymer precursor formed smaller Qdot-solution droplets; the higher flow rate of SDS solution formed smaller ETPTA droplets. Because of the low shrinkage of ETPTA monomer upon polymerization, the microcapsules were formed in the same sizes of the double emulsion droplets. The processes of droplet generation at the T-junction and the Y-junction were recorded by a high-speed camera (Fastcam APX-RS, Photron, Japan) mounted to an inverted microscope (Eclipse *Ti*, Nikon, Japan).

3. Formation of Predefinable Barcodes

Since the ETPTA polymer shell has a high transmittance (>90%) from UV (380 nm) to infrared (800 nm), the UV light used to excite the Qdots in the liquid cores and the emissions from these Qdots can go through the transparent polymer shells. The Qdot-loaded liquid core has a bright emission under UV illumination as shown in Fig. 2(a). The microfluidic method to form the Qdot-encoded microcapsules maintains the Qdots' original characteristics. The Qdot emission peaks are the same as before being encapsulation as shown in Fig. 2(b), and the emission intensity of the Qdot-loaded liquid core is linearly proportional to the Qdot concentration in the liquid cores as shown in Fig. 2(c). Furthermore, we found that the Qdots with different emission peaks can be mixed in a high concentration up to 6 μM without

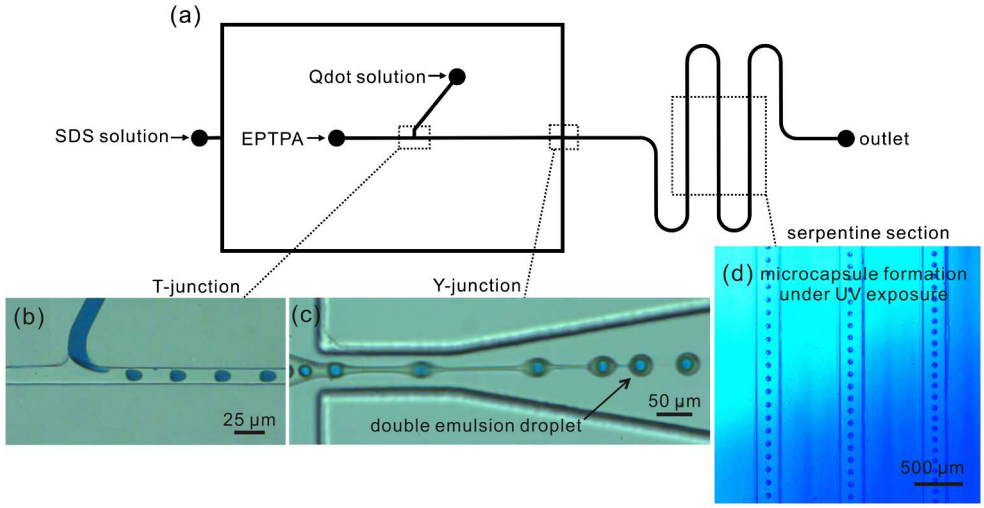

Fig. 1. (Color online) Fabrication of the microcapsules. (a) Schematic diagram of the microfluidic device. (b) T-junction to generate the Qdot-solution droplets. Blue ink is added in the Qdot solution for illustration. (c) Y-junction to generate the double emulsion droplets. (d) The double emulsion droplets queue in the serpentine section under UV exposure to form the microcapsules.

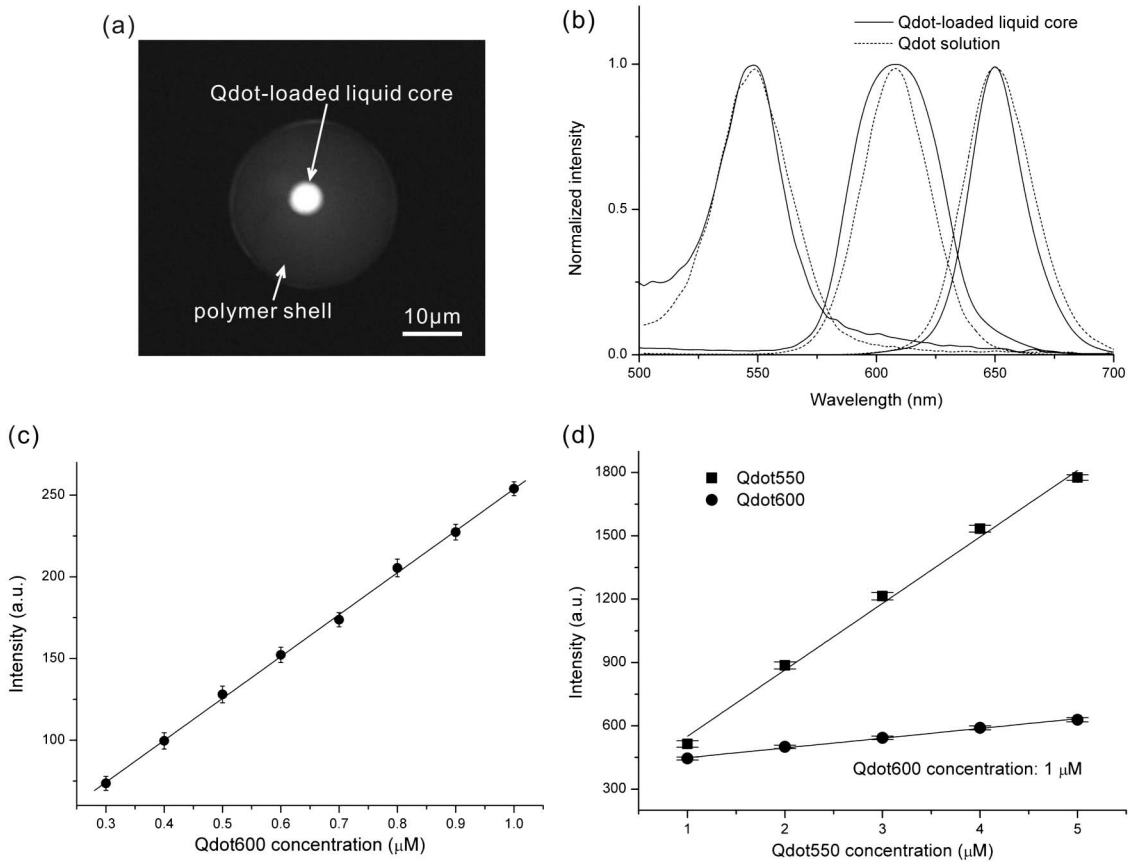

Fig. 2. (a) Fluorescent micrograph of a microcapsule. Its liquid core contains 0.5 μM Qdot600 [7]. (b) The Qdots loaded in the liquid cores maintain their original emission peaks. (c) The emission intensity of the Qdot-loaded liquid core is linearly proportional to the Qdot concentration [7]. (d) Qdot550 and Qdot600 have no interference in their mixtures up to 6 μM. The concentrations of Qdot550 increased from 1 to 5 μM in an increment of 1 μM for these five Qdot solutions. The concentrations of Qdot600 were 1 μM constantly. The exposure times for image capturing were 800 ms for Qdot550 and 100 ms for Qdot600.

FRET. As shown in Fig. 2(d), the emission intensities of Qdot550 in the Qdot mixtures are linearly proportional to their concentrations. It should be noted that the slight increasing emission intensities at 600 nm are due to the spectral overlapping of Qdot550 at 600 nm. Each specific Qdot mixture can create a corresponding specific emission profile for encoding. The colorimetric barcodes can be formed by multiplexing the Qdot emission peaks and concentrations in the liquid cores, which require no interrogation of the specificities of their fluorescent profiles. The barcodes in the microcapsules can be predefined directly and only by the compositions of the Qdot mixtures in the liquid cores [7].

4. Identification Method and Algorithm

Previous identification methods used spectrometers to record the emission spectra of Qdot-encoded microparticles. To identify the barcodes multiplexed by colors and emission intensities, deconvolution algorithms were developed to separate the emissions of Qdots in different colors from the overlapped spectra of Qdot mixtures [5,15]. However, the time-consuming spectrum-recording process and the computationally intensive deconvolution algorithms are not suitable for high-throughput screening applications. We proposed a simple and express identification algorithm for our predefinable barcodes by recording the emission intensities of Qdot-encoded microcapsules at the respective Qdot emission peaks. Here the emission intensities of the colorimetric Qdot barcodes were recorded by a monochromatic CCD camera (RETIGE EXi, Qimaging, Canada) with narrow bandpass optical filters (FWHM, 10 nm; Thorlabs, USA) mounted to a microscope (Eclipse LV-100, Nikon, Japan). UV light from a mercury lamp (100 W) equipped to the microscope was used to excite the Qdots.

Since the Qdots emitting in different colors have no interference in the liquid cores, the emission intensity of the Qdot-encoded microcapsule, $F(\omega)$, at a certain Qdot emission peak, ω, is a linear superposition of the emission intensities from the Qdots in different colors:

$$F(\omega) = a \cdot f_{550}(\omega) + b \cdot f_{600}(\omega) + c \cdot f_{650}(\omega), \qquad (1)$$

where $f_{550}(\omega)$, $f_{600}(\omega)$, and $f_{650}(\omega)$ are the emission intensities of intensity-reference microcapsules at emission peak ω. Three batches of microcapsules containing Qdot550, Qdot600, and Qdot650, in known

concentrations were made as the intensity-reference microcapsules. a, b, and c represent relative composition of a Qdot mixture to the intensity references. The array (a, b, c) is used as the name of the barcode. The emission intensities of these intensity-reference microcapsules at the three Qdot emission peaks can be expressed by following *intensity-reference matrix*, $\boldsymbol{D}$:

$$\boldsymbol{D} = \begin{pmatrix} f_{550}(550) & f_{550}(600) & f_{550}(650) \\ f_{600}(550) & f_{600}(600) & f_{600}(650) \\ f_{650}(550) & f_{650}(600) & f_{650}(650) \end{pmatrix}. \quad (2)$$

The emission intensities of the Qdot-encoded microcapsule at these three Qdot emission peaks can be expressed by the following *barcode emission matrix*, $\boldsymbol{F}$,

$$\boldsymbol{F} = (F(550) \quad F(600) \quad F(650)), \quad (3)$$

because $F(550)$, $F(600)$, and $F(650)$ can be written in the format as Eq. (1), respectively. The array (a, b, c) can be calculated after $\boldsymbol{F}$ and $\boldsymbol{D}$ are acquired from the fluorescent micrographs of encoded microcapsules:

$$(a \quad b \quad c) = \boldsymbol{F} \cdot \boldsymbol{D}^{-1}. \quad (4)$$

This simple and express algorithm takes account of the spectral overlapping between the Qdots emitting in different colors, which can get the same results as the complicated deconvolution algorithm for the spectrum-based identification method for our predefinable barcodes.

5. Case Study and Discussion

We made a batch of Qdot-encoded microcapsules, the liquid cores of which contain Qdot550, Qdot600, and Qdot650 in concentrations of 5, 0.5, and 0.3 μM, respectively. Our previous investigation indicated that the barcode readout errors are mainly attributed to spectral overlapping and emission intensity variations of the Qdots emitting in different colors. To reduce the adverse effects of spectral overlapping and Qdot emission intensity variations, the intensity-reference microcapsules were made by 5 μM Qdot550, 0.1 μM Qdot600, and 0.1 μM Qdot650, whose emission intensity variations were within an order of magnitude. According to the compositions of this Qdot mixture and the intensity references, the ideal result of barcode identification should be (1, 5, 3). The fluorescent spectrum of the Qdot-encoded microcapsules can be captured for the spectrum-based identification method by a hyperspectral imaging system such as the confocal laser scanning microscope (LSM710, Carl Zeiss, Germany), as shown in Fig. 3(a). Using our proposed identification method, the emission intensities of the Qdot-encoded microcapsule and the intensity-reference microcapsules at the Qdot emission peaks were recorded as a bar chart in Fig. 3(b). The barcode calculated by the simple and express algorithm was (1.02, 4.86, 2.94).

Using the fluorescence microscope described above, 0.1 μM Qdot550, 0.05 μM Qdot600, and 0.02 μM Qdot650 can create discernible intensity gradients. Therefore, the discernible relative concentration gradients of Qdot550, Qdot600, and Qdot650 are 0.02, 0.5, and 0.2, respectively. Theoretically, a barcode can be identified if the absolute error of calculated result is within (0.01, 0.25, 0.1). If the maximum total Qdot concentration without FRET is set at 6 μM, 42,874 barcodes can be created by mixing Qdot550, Qdot600, and Qdot650. (The estimation of coding capacity is $m^n - 1$. m is the number of intensity gradients and n is the number of colors. $0.1m + 0.05m + 0.02m \le 6$, $m = 35$, and the coding capacity is $35^3 - 1 = 42874$.) However, the actual number of disenable intensity gradients and the actual coding capacity are substantially less than the above estimations. Taking the above calculated barcode for example, its absolute error is (0.02, 0.14, 0.06), and it will be recognized mistakenly as the ideal barcode of (1.02, 5, 3) but not (1, 5, 3). The Qdot550 concentration gradient should be increased more than 0.2 μM to avoid the mistaken identification. Actually, the discernible Qdot550 concentration gradient is much higher in other instances when the Qdot550 is in a lower concentration

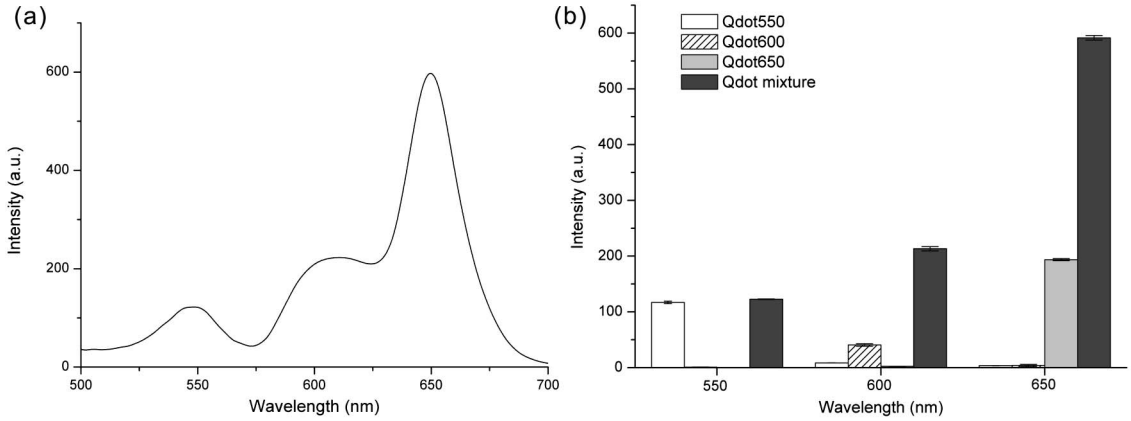

Fig. 3. (a) Fluorescent spectrum of the encoded microcapsule. (b) Bar chart of emission intensities of the encoded microcapsule and the intensity-reference microcapsules. The exposure time for image capturing was 100 ms.

in the Qdot mixture. The Qdot spectral overlapping and variations of emission intensities have significantly adverse effects on the actual coding capacity.

6. Conclusions

In summary, we developed predefinable colorimetric barcodes by loading aqueous Qdot mixtures as liquid cores into monodispersed microcapsules. The colorimetric barcodes can be formed simply by multiplexing the Qdot emission peaks and concentrations, which are only determined by the compositions of Qdot mixtures in the liquid cores of microcapsules. These predefinable colorimetric Qdot barcodes can be identified easily by recording their emission intensities at respective Qdot emission peaks with a simple and express data processing algorithm. Taking advantage of the simplicity of this barcode identification algorithm, it is very promising to use a flow cytometer for barcode identification and assay result analysis with a high-throughput capability up to 4000–20,000 per second.

Bo Wu would like to acknowledge the Ph.D. scholarship from Nanyang Technological University.

References

1. U. Resch-Genger, M. Grabolle, S. Cavaliere-Jaricot, R. Nitschke, and T. Nann, "Quantum dots versus organic dyes as fluorescent labels," Nat. Methods **5**, 763–775 (2008).
2. I. L. Medintz, H. T. Uyeda, E. R. Goldman, and H. Mattoussi, "Quantum dot bioconjugates for imaging, labelling and sensing," Nat. Mater. **4**, 435–446 (2005).
3. M. Y. Han, X. H. Gao, J. Z. Su, and S. Nie, "Quantum-dot-tagged microbeads for multiplexed optical coding of biomolecules," Nat. Biotechnol. **19**, 631–635 (2001).
4. D. Y. Wang, A. L. Rogach, and F. Caruso, "Semiconductor quantum dot-labeled microsphere bioconjugates prepared by stepwise self-assembly," Nano Lett. **2**, 857–861 (2002).
5. J. A. Lee, S. Mardyani, A. Hung, A. Rhee, J. Klostranec, Y. Mu, D. Li, and W. C. W. Chan, "Toward the accurate read-out of quantum dot barcodes: design of deconvolution algorithms and assessment of fluorescence signals in buffer," Adv. Mater. **19**, 3113–3118 (2007).
6. S. Fournier-Bidoz, T. L. Jennings, J. M. Klostranec, W. Fung, A. Rhee, D. Li, and W. C. W. Chan, "Facile and rapid one-step mass preparation of quantum-dot barcodes," Ang. Chem. Int. Ed. **47**, 5577–5581 (2008).
7. B. Wu and H.-Q. Gong, "Fluorescence-profile pre-definable quantum-dot barcodes in liquid-core microcapsules," Microfluid. Nanofluid. **13**, 909–917 (2012).
8. A. S. Utada, E. Lorenceau, D. R. Link, P. D. Kaplan, H. A. Stone, and D. A. Weitz, "Monodisperse double emulsions generated from a microcapillary device," Science **308**, 537–541 (2005).
9. Z. H. Nie, S. Q. Xu, M. Seo, P. C. Lewis, and E. Kumacheva, "Polymer particles with various shapes and morphologies produced in continuous microfluidic reactors," J. Am. Chem. Soc. **127**, 8058–8063 (2005).
10. B. Wu and H.-Q. Gong, "Formation of fully closed microcapsules as microsensors by microfluidic double emulsion," Microfluid. Nanofluid., 1–8 (2012).
11. J. Inglese, R. L. Johnson, A. Simeonov, M. H. Xia, W. Zheng, C. P. Austin, and D. S. Auld, "High-throughput screening assays for the identification of chemical probes," Nat. Chem. Biol. **3**, 466–479 (2007).
12. R. Wilson, A. R. Cossins, and D. G. Spiller, "Encoded microcarriers for high-throughput multiplexed detection," Ang. Chem. Int. Ed. **45**, 6104–6117 (2006).
13. Y. N. Xia and G. M. Whitesides, "Soft lithography," Annu. Rev. Mater. Sci. **28**, 153–184 (1998).
14. W. W. Yu, L. H. Qu, W. Z. Guo, and X. G. Peng, "Experimental determination of the extinction coefficient of CdTe, CdSe, and CdS nanocrystals," Chem. Mater. **15**, 2854–2860 (2003).
15. K. C. Goss, G. G. Messier, and M. E. Potter, "Data detection algorithms for multiplexed quantum dot encoding," Opt. Express **20**, 5762–5774 (2012).